



Research article

Distributed optimization of nonlinear singularly perturbed multi-agent systems via a small-gain approach and sliding mode control

Qian Li¹, Zhenghong Jin^{2,3,*}, Linyan Qiao¹, Aichun Du⁴ and Gang Liu¹

¹ School of Vehicle and Transportation Engineering, Henan Institute of Technology, Xinxiang 453003, China

² School of Electrical and Electronic Engineering, Nanyang Technological University, 639798, Singapore

³ State Key Laboratory of Industrial Control Technology, Zhejiang University, Hangzhou 310027, China

⁴ School of Mechanical and Electrical Department, Hami Vocational and Technical College, Hami 839000, China

* **Correspondence:** Email: zhjin_neu@163.com; Tel: +8613840161912.

Abstract: This paper addressed the challenging problem of distributed optimization for nonlinear singular perturbation multi-agent systems. The main focus lies in steering the system outputs toward the optimal points of a globally objective function, which was formed by the combination of several local functions. To achieve this objective, the singular perturbation multi-agent system was initially decomposed into fast and slow subsystems. Compared to traditional methods, robustness in reference-tracking signals was ensured through the design of fast-slow sliding mode controllers. Additionally, our method ensured robustness against errors between reference signals and optimal values by employing a distributed optimizer to generate precise reference signals. Furthermore, the stability of the entire closed-loop system was rigorously guaranteed through the application of the small-gain theorem. To demonstrate the efficacy of the proposed approach, a numerical example was presented, providing empirical validation of its effectiveness in practical scenarios.

Keywords: distributed optimization; robust stability; singularly perturbed systems; small-gain theorem; sliding mode control

Mathematics Subject Classification: 93A16, 93C10, 93C70

1. Introduction

1.1. Motivation

Nonlinear singularly perturbed systems represent a class of dynamic systems where certain components exhibit significantly different time scales. These systems are ubiquitous in various fields, including control theory, engineering, and natural sciences [1–5]. The presence of multiple timescales introduces challenges in analysis and control, as traditional methods may fail to capture the system's intricate behavior accurately. Singular perturbation theory provides a powerful framework for studying such systems by decomposing them into fast and slow subsystems. This decomposition enables the analysis of the system's behavior on different timescales separately, leading to simplified models and insights into system dynamics.

1.2. Related work

In recent years, there has been growing interest in nonlinear singularly perturbed systems due to their relevance in practical applications and their rich mathematical properties. Researchers have explored various aspects of these systems, including stability analysis [6, 7], control design [8], and adaptive techniques [9], aiming to develop robust and efficient control strategies capable of handling the inherent complexities. In [10], the issue of finite-time fuzzy control for discrete-time nonlinear singularly perturbed systems with input constraints is addressed, focusing on establishing conditions for state boundedness using matrix inequality techniques and overcoming issues related to small singularly perturbed parameters. In [11], the fuzzy-model-based approach is proposed for optimizing nonlinear Markov jump singularly perturbed systems using reinforcement learning, featuring robust offline and online parallel learning algorithms that ensure convergence and efficacy. In [12], a composite controller is designed for fast sampling singularly perturbed systems, designed without full system dynamics, improving convergence speed and eliminating the need for a stabilizing control strategy. The integration of multi-agent systems with singularly perturbed dynamics presents a compelling area of research with profound implications for the design and control of complex distributed systems [13]. In these systems, the agents may exhibit fast and slow dynamics, resulting in intricate interactions and nontrivial behaviors. Understanding and effectively controlling such systems pose significant challenges, as traditional control techniques may fail to capture their dynamics accurately.

Distributed optimization is a method of cooperative optimization among multiple distributed agents to achieve global optimization objectives [14–17]. Nonlinear singularly perturbed systems are a class of dynamic systems characterized by significantly different timescales and nonlinear properties. Combining these two fields, distributed optimization and nonlinear singularly perturbed systems, can be applied in various domains such as information fusion, network flow optimization, and multi-robot coordination. Against this backdrop, researchers have begun to focus on how to effectively optimize nonlinear singularly perturbed systems in distributed environments [18, 19]. This optimization problem is challenging because the complexity of the system and multiple timescales can render traditional optimization techniques ineffective or suboptimal. Therefore, developing new distributed optimization algorithms to address these issues becomes crucial. Nonlinear small-gain theorem [20, 21] is an important tool for analyzing the interaction between distributed optimization and singular perturbation

systems with multiple timescales.

The small-gain theorem stands as a cornerstone in control theory, offering profound insights into the stability analysis of interconnected systems [22, 23]. This theorem provides a powerful tool for assessing the stability of interconnected systems by establishing a connection between the gains of individual subsystems and the overall stability of the interconnected system. At its core, the nonlinear small-gain theorem asserts that if the gains of interconnected subsystems are suitably bounded, then the overall system will exhibit stability, even if individual subsystems may be unstable. This property is particularly valuable in the analysis of complex systems composed of interconnected components with varying dynamics and behaviors.

This paper aims to explore the application of distributed optimization in nonlinear singularly perturbed systems via the small-gain theorem and sliding mode control. We will investigate how to leverage cooperation among distributed agents to effectively optimize performance metrics of such systems, such as stability, convergence, and robustness. By combining the theories and methods of distributed optimization and nonlinear singularly perturbed systems, we aim to provide new insights and solutions for addressing complex distributed system problems in practice.

1.3. Contributions

The main contributions of this study are as follows:

- (1) Compared with distributed optimization multi-agent systems [24, 25], our paper considers the more general multi-timescales singular perturbation systems, which have broader prospects for practical applications.
- (2) In contrast to a previous study [26], our paper avoids assuming input-to-state stability (ISS) properties of the reference signal and instead achieves reference signal tracking by designing sliding mode controllers with fast and slow timescales.
- (3) Compared with previously reported approaches [27], our proposed algorithm can avoid the use of the analytical form of the gradient function and only relies on the gradient function values to achieve the optimization objective. Furthermore, the convergence and robustness of the distributed optimization algorithm can be guaranteed.

1.4. Structure and notation

The rest of the paper is organized as follows. In Section 2, we present the problem formulation of this paper. The proof of the main result is placed in Sections 3 and 4. In Section 5, we employ numerical examples to verify the effectiveness of the theoretical result. Section 6 concludes this paper.

Notations: Throughout this paper, \mathbb{R}^+ denotes the positive real number set. We use $\mathbf{1}_N$ and \mathbf{I}_N to represent the N -dimensional vector $[1, \dots, 1]^T$ and N -dimensional identity matrix, respectively. We use $|\cdot|$ and \otimes to represent the Euclidean norm for real vectors and the Kronecker product, respectively. The function sgn takes the sign of real values, that is, $\text{sgn}(r) = 1$ if $r > 0$, $\text{sgn}(r) = -1$ if $r < 0$, and $\text{sgn}(r) = 0$ if $r = 0$. We use Id to represent the identity function on \mathbb{R}_+ . For a matrix A , A^\dagger denotes the Moore-Penrose pseudo-inverse of the matrix A . $f \circ g$ denotes the composition of appropriately defined functions f and g . $\|z\|_T = \sup_{t \in T} |z(t)|$ denotes the supremum norm of a continuous function $z(t) : \mathbb{R}^+ \rightarrow \mathbb{R}^n$.

Given continuous function $\alpha : \mathbb{R}^+ \rightarrow \mathbb{R}^+$ and $\beta : \mathbb{R}^+ \times \mathbb{R}^+ \rightarrow \mathbb{R}^+$, $\alpha(0) = 0$, it follows that:

- The function α is called:
 - (1) positive definite if $\alpha(s) > 0$ ($s > 0$);
 - (2) a class \mathcal{K} function ($\alpha \in \mathcal{K}$) if α is a strictly increasing function;
 - (3) a class \mathcal{K}_∞ function ($\alpha \in \mathcal{K}_\infty$) if α is \mathcal{K} function and satisfies $\lim_{s \rightarrow \infty} \alpha(s) = \infty$.
- The function β is called a class \mathcal{KL} function ($\beta \in \mathcal{KL}$) if $\beta(\cdot, t)$ is a class \mathcal{K} function ($t \in \mathbb{R}^+$) and $\beta(s, \cdot)$ is a decreasing function satisfying $\lim_{t \rightarrow \infty} \beta(s, t) = 0$.

2. Preliminaries and problem formulation

Consider the following multi-agent system characterized by singular perturbations:

$$\dot{x}_i = f_{1i}(x_i) + F_{1i}(x_i)z_i + g_{1i}(x_i)u_i, \quad (2.1)$$

$$\varepsilon \dot{z}_i = f_{2i}(x_i) + F_{2i}(x_i)z_i + g_{2i}(x_i)u_i, \quad (2.2)$$

$$y_i = \psi_i(x_i, z_i), \quad (2.3)$$

for $i \in \mathcal{N} = \{1, \dots, N\}$, where $x_i \in \mathbb{R}^{n_{xi}}$ and $z_i \in \mathbb{R}^{n_{zi}}$ are the slow and fast state, respectively. ε is a small positive constant, $u_i \in \mathbb{R}^{n_{ui}}$ is the control input, and $y_i \in \mathbb{R}^{n_y}$ is the output. $f_{1i} : \mathbb{R}^{n_{xi}} \rightarrow \mathbb{R}^{n_{xi}}$, $F_{1i} : \mathbb{R}^{n_{xi}} \rightarrow \mathbb{R}^{n_{xi} \times n_{zi}}$, $g_{1i} : \mathbb{R}^{n_{xi}} \rightarrow \mathbb{R}^{n_{xi} \times n_{ui}}$, $f_{2i} : \mathbb{R}^{n_{xi}} \rightarrow \mathbb{R}^{n_{zi}}$, $F_{2i} : \mathbb{R}^{n_{xi}} \rightarrow \mathbb{R}^{n_{zi} \times n_{zi}}$, and $g_{2i} : \mathbb{R}^{n_{xi}} \rightarrow \mathbb{R}^{n_{zi} \times n_{ui}}$ represent the system dynamics. $\psi_i : \mathbb{R}^{n_{xi}} \times \mathbb{R}^{n_{zi}} \rightarrow \mathbb{R}^{n_y}$ represents the output map. Specifically, ψ_i is a linear function with respect to x_i and z_i . Suppose f_{1i} , f_{2i} , and all elements in matrices g_{1i} , g_{2i} , F_{1i} , and F_{2i} are smooth bounded functions, and F_{2i} is a nonsingular matrix for $x_i \in \mathbb{R}^{n_{xi}}$. Let $x_i(t_0) = x_{i0}$, $z_i(t_0) = z_{i0}$, where t_0 denotes initial time. Notice that the outputs of all outputs of the agents have the same dimension while their states could have different dimensions.

Consider the optimization problem

$$\min_{r \in \mathbb{R}^{n_y}} c(r), c(r) = \sum_{i \in \mathcal{N}} c_i(r) \quad (2.4)$$

for $i \in \mathcal{N}$, where $c_i : \mathbb{R}^{n_y} \rightarrow \mathbb{R}$ are differentiable functions, which are called local objective functions. Define $y^* \in \mathbb{R}^{n_y}$ as the global minimizer of c .

Next, we provide a description of the problem that this paper aims to address.

Problem: The objective of this paper is to design a distributed controller for the multi-agent system with singular perturbation (2.1)–(2.3) to steer the outputs y_i of all agents to the optimal solution y^* of optimization problem (2.4). Specifically,

$$\lim_{t \rightarrow \infty} y_i(t) = y^*, \forall i \in \mathcal{N} \quad (2.5)$$

where y^* can be either a constant or a continuous function of time and \dot{y}^* is any measurable and locally essentially bounded.

The following assumptions will be made regarding the local objective functions and the state functions.

Assumption 2.1. $f_{1i}(0) = 0$, $f_{2i}(0) = 0$, and for $u_i = 0$, $i \in \mathcal{N}$, the origin $(0, 0)$ is an isolated equilibrium point. The equation $f_{2i}(x_i) + F_{2i}(x_i)z_i + g_{2i}(x_i)u_i = 0$ of the multi-agent system (2.1) has a unique continuous solution over $[0, +\infty)$, which is described:

$$z_i = h_i(x_i, u_i), \quad (2.6)$$

where $h_i : \mathbb{R}^{n_{xi}} \times \mathbb{R}^{n_{ui}} \rightarrow \mathbb{R}^{n_{zi}}$.

Assumption 2.2. For each $i \in \mathcal{N}$, c_i is ω -strongly convex over \mathbb{R}^{n_y} with constant $\omega > 0$, and its gradient ∇c_i is ϑ -Lipschitz with constant $\vartheta > 0$. Specifically,

$$(\nabla^T c_i(\xi_1) - \nabla^T c_i(\xi_2))(\xi_1 - \xi_2) \geq \omega|\xi_1 - \xi_2|^2, \quad (2.7)$$

$$|\nabla c_i(\xi_1) - \nabla c_i(\xi_2)| \leq \vartheta|\xi_1 - \xi_2|. \quad (2.8)$$

for any $\xi_1, \xi_2 \in \mathbb{R}^{n_y}$.

Remark 2.1. Based on the Assumption 2.2, we have that (2.7) and (2.8) hold. Therefore,

$$(\nabla^T c(\xi_1) - \nabla^T c(\xi_2))(\xi_1 - \xi_2) = (\nabla^T \sum_{i \in \mathcal{N}} c_i(\xi_1) - \nabla^T \sum_{i \in \mathcal{N}} c_i(\xi_2))(\xi_1 - \xi_2) \geq N\omega|\xi_1 - \xi_2|^2,$$

and

$$|\nabla c(\xi_1) - \nabla c(\xi_2)| = |\nabla \sum_{i \in \mathcal{N}} c_i(\xi_1) - \nabla \sum_{i \in \mathcal{N}} c_i(\xi_2)| \leq N\vartheta|\xi_1 - \xi_2|,$$

for any $\xi_1, \xi_2 \in \mathbb{R}^{n_y}$, that is, c is strongly convex with the constant $N\omega$ and ∇c is ϑ -Lipschitz with the constant $N\vartheta$, which guarantees the existence of the unique global minimizer.

The information exchange topology of the multi-agent system is described by a digraph $\mathcal{G} = \{\mathcal{N}, \mathcal{B}, \mathcal{A}\}$. Specifically, each agent is represented by a node in \mathcal{G} , and $(i, j) \in \mathcal{B}$ if the information of agent i is available to agent j . The element of $\mathcal{A} = [a_{ij}]$ denotes the adjacency matrix weight of edge (i, j) .

Assumption 2.3. The digraph \mathcal{G} is quasi-strongly connected (QSC) and weight-balanced.

Through distributed optimal output agreement, we aim to ensure that each agent's control incorporates both local information, denoted as $\nabla c_i(y_i)$, and exchanged information from neighboring agents. The objective is to maintain the boundedness of all signals within the closed-loop system and guide the agents' outputs toward the optimal point.

This paper aims to pioneer the development of a novel class of distributed optimal output agreement strategies within multi-agent systems, leveraging a sophisticated two-time scale framework. At its core, the distributed optimal coordinator harnesses available data intelligently, crafting optimal reference signals y_i^r tailored for each agent's individual requirements. Following this, a meticulously designed two timescale reference-tracking composite sliding mode controller assumes the helm as the agents' primary controller, orchestrating precise maneuvers to faithfully track these reference signals.

For each agent, the reference-tracking composite sliding mode controllers will be designed in the form of

$$\dot{\tilde{\xi}}_i = \tilde{f}_{ci}(\tilde{\xi}_i, x_i, z_i, \varepsilon, y_i^r), \quad (2.9)$$

$$u_i = \tilde{g}_{ci}(\tilde{\xi}_i, x_i, z_i, \varepsilon, y_i^r), \quad (2.10)$$

where $\tilde{\xi}_i \in \mathbb{R}^{m_i}$ is the internal state, and $\tilde{f}_{ci} : \mathbb{R}^{m_i} \times \mathbb{R}^{n_{xi}} \times \mathbb{R}^{n_{zi}} \times \mathbb{R} \times \mathbb{R}^{n_y} \rightarrow \mathbb{R}^{m_i}$ and $\tilde{g}_{ci} : \mathbb{R}^{m_i} \times \mathbb{R}^{n_{xi}} \times \mathbb{R}^{n_{zi}} \times \mathbb{R} \times \mathbb{R}^{n_y} \rightarrow \mathbb{R}^{n_{ui}}$ represent the dynamics and the output map of the control law, respectively. Moreover, \tilde{f}_{ci} is designed to be locally Lipschitz, $i \in \mathcal{N}$.

3. Distributed optimal coordinators

In an ideal scenario, if the controlled agents can effectively track any reference signal, the optimal output agreement problem simplifies to determining optimal reference signals for the agents. This section centers on designing distributed optimal coordinators, assuming the reference-tracking capability of the controlled agents.

3.1. Two timescales multi-agent systems

According to Eqs (2.1)–(2.3) and [28], the slow subsystem is written as

$$\dot{x}_{si} = f_i(x_{si}) + g_i(x_{si})u_{si}, \quad (3.1)$$

$$z_{si} = h_i(x_{si}, u_{si}) := -F_{2i}^{-1}(x_{si}) [f_{2i}(x_{si}) + g_{2i}(x_{si})u_{si}(x_{si})], \quad (3.2)$$

$$f_i(x_{si}) := f_{1i}(x_{si}) - F_{1i}(x_{si})F_{2i}^{-1}(x_{si})f_{2i}(x_{si}), \quad (3.3)$$

$$g_i(x_{si}) := g_{1i}(x_{si}) - F_{1i}(x_{si})F_{2i}^{-1}(x_{si})g_{2i}(x_{si}), \quad (3.4)$$

for $i \in \mathcal{N}$, $x_{si}(t_0) = x_{si0}$, where $x_{si} \in \mathbb{R}^{n_{xi}}$, $z_{si} \in \mathbb{R}^{n_{zi}}$, and $u_{si} \in \mathbb{R}^{n_{ui}}$ represent the slow components of state variables x_i , z_i and u_i , respectively. It is also said to be the reduced system (RS) and is locally Lipschitz.

Define the fast timescale:

$$\tau = \frac{t - t_0}{\varepsilon}. \quad (3.5)$$

Define coordinate transformation $z_{\tau i} = z_i - h_i(x_i, u_i)$, and the singularly perturbed multi-agent systems in (2.1) take the form with the τ timescale

$$\frac{dx_{\tau i}}{d\tau} = \varepsilon [f_{1i}(x_{\tau i}) + F_{1i}(z_{\tau i}) (h_i(x_{\tau i}, u_i) + z_{\tau i}) + g_{1i}(x_{\tau i})u_i], \quad (3.6)$$

$$\begin{aligned} \frac{dz_{\tau i}}{d\tau} = & f_{2i}(x_{\tau i}) + F_{2i}(z_{\tau i}) (h_i(x_{\tau i}, u_i) + z_{\tau i}) + g_{2i}(x_{\tau i})u_i \\ & - \varepsilon \left[\frac{\partial h_i}{\partial x_{\tau i}} (F_{1i}(z_{\tau i}) (h_i(x_{\tau i}, u_i) + z_{\tau i}) + f_{1i}(x_{\tau i}) + g_{1i}(x_{\tau i})u_i) + \frac{\partial h_i}{\partial u_i} \dot{u}_i \right], \end{aligned} \quad (3.7)$$

for $i \in \mathcal{N}$.

When $\varepsilon = 0$, it is obtained that

$$\frac{dz_{\tau i}}{d\tau} = f_{2i}(x_{\tau i}) + F_{2i}(z_{\tau i}) (h_i(x_{\tau i}, u_i) + z_{\tau i}) + g_{2i}(x_{\tau i})u_i. \quad (3.8)$$

It is said to be the boundary layer system (BLS) or fast subsystem, which is locally Lipschitz. We can obtain an $O(\varepsilon)$ approximation by setting $\varepsilon = 0$,

$$\frac{d\hat{z}_{\tau i}}{d\tau} = F_{2i}(x_{\tau i}) \hat{z}_{\tau i} + g_{2i}(x_{\tau i}) u_{fi}, \hat{z}_{\tau i}(0) = z_{\tau i}(0) - h_i(x_{i0}, 0). \quad (3.9)$$

Based on above analysis and [29], system (2.1) is rewritten as

$$\dot{x}_i = f_i(x_i) + F_{1i}(x_i)z_{\tau i} + g_i(x_i)u_{si} + g_{1i}(x_i)u_{fi}, \quad (3.10)$$

$$\varepsilon \dot{z}_i = F_{2i}(x_i)z_{\tau i} + g_{2i}(x_i)u_{fi} \quad (3.11)$$

for $i \in \mathcal{N}$, where u_{si} and u_{fi} denote the control law of the slow subsystem and control law of the fast subsystem, respectively. Here, (3.10) and (3.11) describe the interconnection properties between slow and fast variables.

Definition 3.1. *The x_i -subsystem is ISS with z_i , u_{si} , u_{fi} as the inputs and the z_i -subsystem is ISS with x_i , u_{fi} , ε as the inputs. Specifically, there exist $\beta_{xi}, \beta_{zi} \in \mathcal{KL}$, $\gamma_{12}, \gamma_{21}, \gamma_{xi}^{usi}, \gamma_{xi}^{ufi}, \gamma_{zi}^{usi}, \gamma_{zi}^{\varepsilon} \in \mathcal{K}$ such that*

$$|x_i(t)| \leq \max \left\{ \beta_{xi}(|x_{i0}|, t), \gamma_{21}(\|z_i\|_{\infty}), \gamma_{xi}^{usi}(\|u_{si}\|_{\infty}), \gamma_{xi}^{ufi}(\|u_{fi}\|_{\infty}) \right\}, \quad (3.12)$$

$$|z_i(t)| \leq \max \left\{ \beta_{zi}(|z_{i0}|, t), \gamma_{12}(\|x_i\|_{\infty}), \gamma_{zi}^{ufi}(\|u_{fi}\|_{\infty}), \gamma_{zi}^{\varepsilon}(\|\varepsilon\|_{\infty}) \right\} \quad (3.13)$$

for any initial state and any measurable and locally essentially bounded input.

By using fast timescale model transformation, the reference-tracking controllers (2.9) and (2.10) can be written as

$$\dot{\xi}_i = f_{ci}(\xi_i, x_{\tau i}, z_{\tau i}, \varepsilon, y_i^r), \quad (3.14)$$

$$u_i = g_{ci}(\xi_i, x_{\tau i}, z_{\tau i}, \varepsilon, y_i^r), \quad (3.15)$$

where $\xi_i = \tilde{\xi}_i/\varepsilon \in \mathbb{R}^{m_i}$ is the fast timescale internal state of $\tilde{\xi}_i$, and $f_{ci} : \mathbb{R}^{m_i} \times \mathbb{R}^{n_{xi}} \times \mathbb{R}^{n_{zi}} \times \mathbb{R} \times \mathbb{R}^{n_y} \rightarrow \mathbb{R}^{m_i}$ and $g_{ci} : \mathbb{R}^{m_i} \times \mathbb{R}^{n_{xi}} \times \mathbb{R}^{n_{zi}} \times \mathbb{R} \times \mathbb{R}^{n_y} \rightarrow \mathbb{R}^{n_{ui}}$ represent the fast timescale dynamics and the output map of the control law, respectively. In addition, f_{ci} is locally Lipschitz function.

Remark 3.1. *In the following section, all reference signals for the output of agent i and the auxiliary states are in τ timescale.*

4. Design of output tracking sliding mode controller

4.1. Slow sliding mode control

For the slow subsystem (3.1), the output tracking integral sliding mode surface is chosen as

$$s_{si}(t) = x_{si} + Ee_{si} + \int_0^t k_{si}x_{si}(\tau)d\tau, \quad (4.1)$$

where $i \in \mathcal{N}$, k_{si} is the parameter to be designed, and $E \in \mathbb{R}^{n_{xi} \times n_y}$ is a constant matrix with $\|E\| = 1$. The output error is $e_{si} = \psi_i(x_{si}, 0) - y_i^r$.

Based the slow subsystem (3.1) and output tracking integral sliding mode surface (4.1), it can be seen that

$$\begin{aligned} \dot{s}_{si}(t) &= \dot{x}_{si} + E\dot{e}_{si} + k_{si}x_{si} \\ &= k_{si}x_{si} + f_i(x_{si}) + g_i(x_{si})u_{si} + E \frac{\partial \psi_i}{\partial x_{si}} (f_i(x_{si}) + g_i(x_{si})u_{si}) - E\dot{y}_i^r. \end{aligned} \quad (4.2)$$

Note that $\frac{\partial \psi_i}{\partial x_{si}}$ is a constant matrix. When the state trajectories of the slow subsystem enter the sliding mode, it has $s_{si}(t) = 0$ and $\dot{s}_{si}(t) = 0$. Consequently, according to $\dot{s}_{si}(t) = 0$ and (4.1), we obtain the following equivalent control law

$$u_{si}^{eq} = \left(\left(\mathbf{I} + E \frac{\partial \psi_i}{\partial x_{si}} \right) g_i(x_{si}) \right)^{\dagger} \left(E\dot{y}_i^r - k_{si}x_{si} - \left(\mathbf{I} + E \frac{\partial \psi_i}{\partial x_{si}} \right) f_i(x_{si}) \right), \quad (4.3)$$

where I denotes the suitable dimensional identity matrix.

Then, by substituting (4.3) into (3.1), the following sliding mode dynamics of the slow subsystem can be obtained:

$$\dot{x}_{si} = f_i(x_{si}) + g_i(x_{si})u_{si}^{eq} = (I + E \frac{\partial \psi_i}{\partial x_{si}})^{-1} (E \dot{y}_i^r - k_{si} x_{si}). \quad (4.4)$$

Theorem 4.1. *The sliding mode dynamics of slow subsystem (4.4) are ISS with the \dot{y}_i^r being taken as the input under output tracking integral sliding mode surface (4.1) if $k_{si} > 0$ holds for $i \in \mathcal{N}$.*

Proof. Consider a Lyapunov function candidate as follows:

$$V_1(t) = \frac{1}{2} x_{si}^T(t) x_{si}(t). \quad (4.5)$$

The time derivative of $V_1(t)$ along the trajectories of system (4.4) is given by

$$\begin{aligned} \dot{V}_1(t) &= x_{si}^T(t) \left((I + E \frac{\partial \psi_i}{\partial x_{si}})^{-1} (E \dot{y}_i^r - k_{si} x_{si}) \right) \\ &\leq - \frac{k_{si}}{\|I + E \frac{\partial \psi_i}{\partial x_{si}}\|} \|x_{si}(t)\|^2 + \frac{\|\dot{y}_i^r\| \|x_{si}(t)\|}{\|I + E \frac{\partial \psi_i}{\partial x_{si}}\|}. \end{aligned} \quad (4.6)$$

Therefore, we have

$$\dot{V}_1(t) \leq -\alpha \|x_{si}(t)\|^2 + \frac{\|\dot{y}_i^r\| \|x_{si}(t)\|}{\|1 + \frac{\partial \psi_i}{\partial x_{si}}\|},$$

where $\alpha = \frac{k_{si}}{\|I + E \frac{\partial \psi_i}{\partial x_{si}}\|} > 0$ for any $i \in \mathcal{N}$.

Based on the ISS property [30], the sliding mode dynamics of slow subsystem (4.4) are ISS with the \dot{y}_i^r being taken as the input.

The proof is completed. \square

Remark 4.1. *Theorem 4.1 obtains a sufficient condition $k_{si} > 0$, which guarantees that the sliding mode dynamics of slow subsystem (4.4) are ISS. In most singular perturbation systems, the output ψ_i is a linear function and the partial derivative of ψ_i is constant.*

The following output tracking sliding mode controller with exponential reaching law of the slow subsystem (3.1) is designed:

$$u_{si} = \left(\left(I + E \frac{\partial \psi_i}{\partial x_{si}} \right) g_i(x_{si}) \right)^\dagger \left(E \dot{y}_i^r - k_{si} x_{si} - \left(I + E \frac{\partial \psi_i}{\partial x_{si}} \right) f_i(x_{si}) - \eta(s_{si}) \right) \quad (4.7)$$

for $i \in \mathcal{N}$, where $\eta(s_{si}) = \beta_i s_{si}(t) + \delta_i \text{sgn}(s_{si}(t))$, and β_i and δ_i are two known positive constants. Since the external disturbance and uncertainty of the slow subsystem are not considered in this paper, δ_i can be chosen as 0.

Remark 4.2. *In the actual controller design, since there may be a situation where $x_{si} = 0$, we use $\varsigma I + \left(\left(I + E \frac{\partial \psi_i}{\partial x_{si}} \right) g_i(x_{si}) \right)^\dagger$ instead of $\left(\left(I + E \frac{\partial \psi_i}{\partial x_{si}} \right) g_i(x_{si}) \right)^\dagger$ in the denominator of (4.7), where the ς is a small positive constant. This can avoid the jump of sliding mode controller.*

Theorem 4.2. *The slow subsystem (3.1) can reach the output tracking integral sliding mode surface (4.1) in finite time under the sliding mode controller (4.7).*

Proof. Consider a Lyapunov function candidate as follows:

$$V_2(t) = \frac{1}{2} s_{si}^T(t) s_{si}(t). \quad (4.8)$$

Calculating the time derivative of $V_2(t)$ along the trajectory of system (4.4), we have

$$\dot{V}_2(t) = s_{si}^T(t) \left(k_{si} x_{si} + f_i(x_{si}) + g_i(x_{si}) u_{si} + E \frac{\partial \psi_i}{\partial x_{si}} (f_i(x_{si}) + g_i(x_{si}) u_{si}) - E \dot{y}_i^r \right). \quad (4.9)$$

Substituting (4.7) into (4.9) yields

$$\dot{V}_2(t) = s_{si}^T(t) (-\beta_i s_{si}(t) - \delta_i \text{sgn}(s_{si}(t))) \quad (4.10)$$

$$\leq -\beta_i \|s_{si}(t)\|^2. \quad (4.11)$$

According to the sliding mode control theory, the finite time reachability can be guaranteed, that is, the trajectory of the slow subsystem (3.1) converges to the output tracking integral sliding mode surface (4.1) in finite time and remains thereafter.

The proof is completed. \square

For the slow subsystem, the sliding mode controller (4.7) and output tracking integral sliding mode surface (4.1) are designed such that condition $k_{si} > 0$.

Remark 4.3. *In the previous results related to sliding mode control (see [31–33]), it has been shown that the sliding mode dynamics are asymptotically stable, and it was proven that the system can reach the sliding mode surface in finite time, and then concluded that the system is asymptotically stable under the action of the designed sliding mode controller and sliding mode surface. When considering the slow system, the difference between this paper and the existing results is that by proving that the sliding mode dynamic has the ISS property, and then we obtain the conclusion that the system is ISS under the effect of the designed sliding mode controller and the output tracking sliding surface.*

Examples 4.1. Consider the following multi-agent system with three singular perturbation slow subsystems:

$$\dot{x}_{si} = f_i(x_{si}) + g_i(x_{si}) u_{si}, \quad i = 1, 2, 3, \quad (4.12)$$

$$y_i = \psi_i(x_{si}) \quad (4.13)$$

where $f_1(x_{s1}) = -x_{s1}^2$, $g_1(x_{s1}) = -x_{s1}^2$, $f_2(x_{s2}) = x_{s2}^3$, $g_2(x_{s2}) = -x_{s2}$, $f_3(x_{s3}) = x_{s3}^2$, $g_3(x_{s3}) = \sin(x_{s3}/2)$, $\psi_i(x_{si}) = x_{si} + 0.5$, $i = 1, 2, 3$. The reference signal y_i^r is set as 0.5.

The integral sliding mode surface is designed as

$$s_i = x_{si} + e_{si} + \int_0^t k_{si} x_{si}(\tau) d\tau \quad (4.14)$$

for $i = 1, 2, 3$, where $k_{s1} = 0.2$, $k_{s2} = 0.4$, $k_{s3} = 0.1$. The sliding mode controller is designed as

$$u_{si} = -\frac{k_{si} x_{si}(t) + 2f_i(x_{si}) + \beta_i s_{si}(t) + \delta_i \text{sgn}(s_{si}(t))}{0.1 + 2g_i(x_{si})} \quad (4.15)$$

for $i = 1, 2, 3$, where $\beta_i = 0.1, \delta = 0.2$.

Under integral sliding mode surface (4.14) and (4.15) and $x_{s1}(0) = 1, x_{s2}(0) = -1, x_{s3}(0) = -2$, then we obtain the system state response of the closed-loop system shown in Figure 1. The response of integral sliding mode surface is shown in Figure 2. Figure 3 depicts the response of the controller force. The states of three agents will converge to zero within 40s under the integral sliding mode controller (4.14) and the sliding mode surface (4.15).

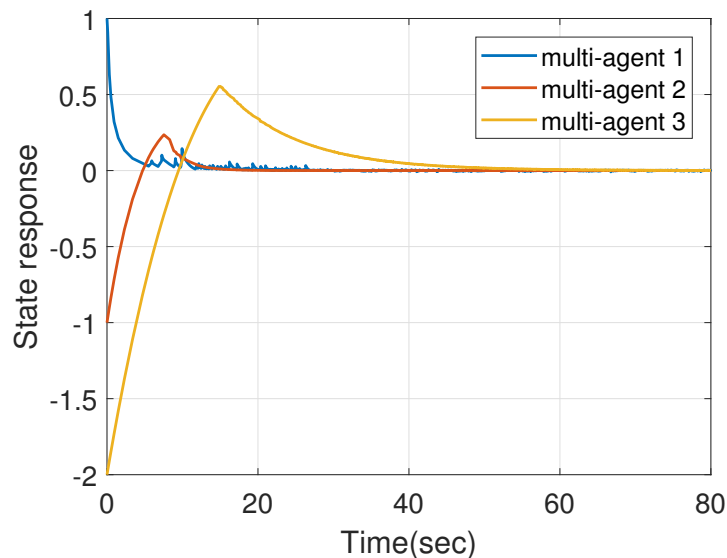


Figure 1. The state responses of the system (4.12).

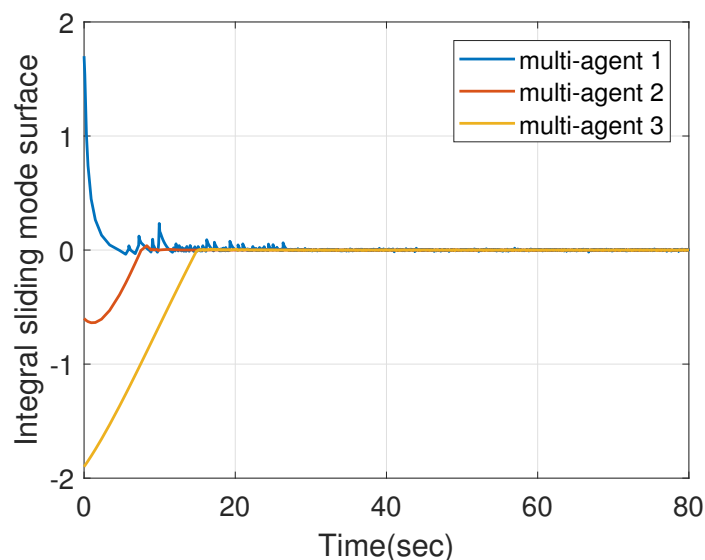


Figure 2. The integral sliding surface $s_i(t)$ (4.14).

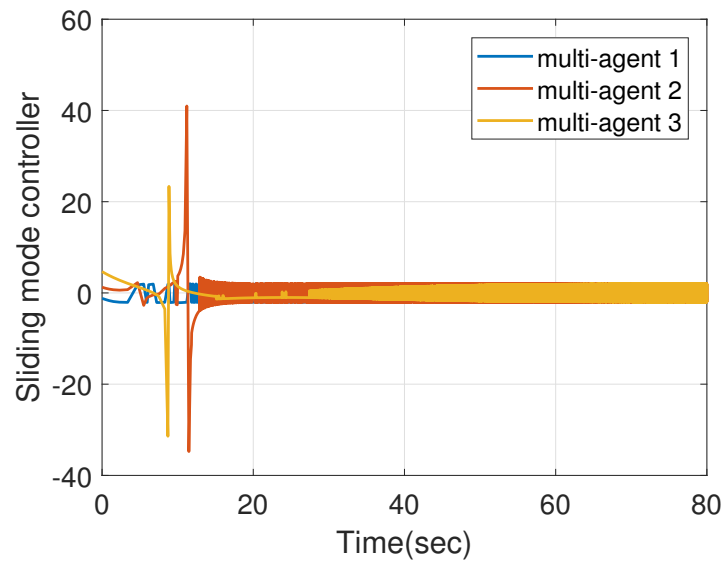


Figure 3. Sliding mode controller $u_i(t)$ (4.15).

4.2. Fast sliding mode control

For the fast subsystem (3.9), the output tracking integral sliding mode surface is chosen as

$$s_{fi}(\tau) = \hat{z}_{\tau i} + \hat{E}e_{fi} + \int_0^\tau k_{fi}\hat{z}_{\tau i}(\xi)d\xi \quad (4.16)$$

for $i \in \mathcal{N}$, k_{fi} is the parameter to be designed. The output error is $e_{fi} = \psi_i(0, \hat{z}_{\tau i}) - y_i^r$, and $\hat{E} \in \mathbb{R}^{n_{zi} \times n_{y_i}}$ is a constant matrix with $\|\hat{E}\| = 1$.

Similarly, based the fast subsystem (3.9) and output tracking integral sliding mode surface (4.16), it can be seen that

$$\begin{aligned} \dot{s}_{fi}(\tau) &= \dot{\hat{z}}_{\tau i} + \hat{E}\dot{e}_{fi} + k_{fi}\hat{z}_{\tau i} \\ &= k_{fi}\hat{z}_{\tau i} + F_{2i}(\hat{z}_{\tau i}) + g_{2i}(\hat{z}_{\tau i})u_{fi} + \hat{E} \frac{\partial \psi_i}{\partial \hat{z}_{\tau i}} (F_{2i}(\hat{z}_{\tau i}) + g_{2i}(\hat{z}_{\tau i})u_{fi}) - \hat{E}\dot{y}_i^r. \end{aligned} \quad (4.17)$$

Based on (4.17), we have

$$\dot{s}_{fi}(\tau) = k_{fi}\hat{z}_{\tau i} + \left(\mathbf{I} + \hat{E} \frac{\partial \psi_i}{\partial \hat{z}_{\tau i}} \right) F_{2i}(\hat{z}_{\tau i}) + \left(\mathbf{I} + \hat{E} \frac{\partial \psi_i}{\partial \hat{z}_{\tau i}} \right) g_{2i}(\hat{z}_{\tau i})u_{fi} - \hat{E}\dot{y}_i^r. \quad (4.18)$$

When the state trajectories of the fast subsystem enter the sliding mode, it has $s_{fi}(\tau) = 0$ and $\dot{s}_{fi}(\tau) = 0$. Consequently, according to $\dot{s}_{fi}(\tau) = 0$ and (4.18), we obtain the following equivalent control law:

$$u_{fi}^{eq} = \left(\left(\mathbf{I} + \hat{E} \frac{\partial \psi_i}{\partial \hat{z}_{\tau i}} \right) g_{2i}(\hat{z}_{\tau i}) \right)^\dagger \left(\hat{E}\dot{y}_i^r - k_{fi}\hat{z}_{\tau i} - \left(\mathbf{I} + \hat{E} \frac{\partial \psi_i}{\partial \hat{z}_{\tau i}} \right) F_{2i}(\hat{z}_{\tau i}) \right). \quad (4.19)$$

Then, by substituting (4.19) into (3.9), the following sliding mode dynamics of the fast system can be obtained:

$$\dot{\hat{z}}_{\tau i} = F_{2i}(\hat{z}_{\tau i}) + g_{2i}(\hat{z}_{\tau i})u_{fi}^{eq} = \left(\mathbf{I} + \hat{E} \frac{\partial \psi_i}{\partial \hat{z}_{\tau i}} \right)^{-1} (\hat{E}\dot{y}_i^r - k_{fi}\hat{z}_{\tau i}). \quad (4.20)$$

Theorem 4.3. *The sliding mode dynamics of fast subsystem (4.20) are ISS with the \dot{y}_i^r being taken as the input under output tracking integral sliding mode surface (4.16) if there exists $k_{fi} > 0$ for $i \in \mathcal{N}$.*

Proof. Consider a Lyapunov function candidate as follows:

$$V_1(\tau) = \frac{1}{2} \hat{z}_{\tau i}^T(\tau) \hat{z}_{\tau i}(\tau). \quad (4.21)$$

The proof is a similar version of proof of Theorem 4.1, and it will not be explained. Based on the ISS property [30], the sliding mode dynamics of fast subsystem (4.20) are ISS with the \dot{y}_i^r being taken as the input.

The proof is completed. \square

Remark 4.4. *Theorem 4.3 obtains a sufficient condition $k_{fi} > 0$, which guarantees the sliding mode dynamics of fast subsystem (4.20) are ISS.*

The following output tracking sliding mode controller with exponential reaching law of the fast subsystem (3.9) is designed:

$$u_{fi} = \left(\left(\mathbf{I} + \hat{E} \frac{\partial \psi_i}{\partial \hat{z}_{\tau i}} \right) g_{2i}(\hat{z}_{\tau i}) \right)^\dagger \left(\hat{E} \dot{y}_i^r - k_{fi} \hat{z}_{\tau i} - \left(\mathbf{I} + \hat{E} \frac{\partial \psi_i}{\partial \hat{z}_{\tau i}} \right) F_{2i}(\hat{z}_{\tau i}) - \eta(s_{fi}) \right), \quad (4.22)$$

where $\eta(s_{fi}) = \beta_i s_{fi}(t) - \delta_i \text{sgn}(s_{fi}(t))$, and β_i and δ_i are two known positive constants for $i \in \mathcal{N}$.

Remark 4.5. *Similar to Remark 4.4, since there may be a situation where $g_{2i}(\hat{z}_{\tau i}) = 0$, we use $\zeta \mathbf{I} + \left(\mathbf{I} + \hat{E} \frac{\partial \psi_i}{\partial \hat{z}_{\tau i}} \right) g_{2i}(\hat{z}_{\tau i})$ instead of $\left(\mathbf{I} + \hat{E} \frac{\partial \psi_i}{\partial \hat{z}_{\tau i}} \right) g_{2i}(\hat{z}_{\tau i})$ in the denominator of (4.22), where the ζ is a small positive constant.*

Theorem 4.4. *The fast subsystem (3.9) can reach the output tracking integral sliding mode surface (4.16) in finite time under the sliding mode controller (4.22).*

Proof. Consider a Lyapunov function candidate as follows:

$$V_2(\tau) = \frac{1}{2} s_{fi}^T(\tau) s_{fi}(\tau). \quad (4.23)$$

Calculating the time derivative of $V_2(\tau)$ along the trajectory of system (4.20), we have

$$\dot{V}_2(\tau) = s_{fi}^T(\tau) \left(\begin{array}{l} k_{fi} \hat{z}_{\tau i} + F_{2i}(\hat{z}_{\tau i}) + g_{2i}(\hat{z}_{\tau i}) u_{fi} \\ + \hat{E} \frac{\partial \psi_i}{\partial \hat{z}_{\tau i}} (F_{2i}(\hat{z}_{\tau i}) + g_{2i}(\hat{z}_{\tau i}) u_{fi}) - \hat{E} \dot{y}_i^r \end{array} \right). \quad (4.24)$$

Substituting (4.22) into (4.24) yields

$$\dot{V}_2(\tau) = s_{fi}^T(\tau) \left(-\beta_i s_{fi}(\tau) - \delta_i \text{sgn}(s_{fi}(\tau)) \right) \quad (4.25)$$

$$\leq -\beta_i \|s_{fi}(\tau)\|^2. \quad (4.26)$$

According to the sliding mode theory, the finite time reachability can be guaranteed, that is, the trajectory of the fast subsystem (3.9) converges to the output tracking integral sliding mode surface (4.16) in finite time and remains thereafter.

The proof is completed. \square

For the fast subsystem, the sliding mode controller (4.22) and output tracking integral sliding mode surface (4.16) are designed such that condition $k_{fi} > 0$.

4.3. A gradient-based design and its robustness

This subsection presents a category of distributed optimal coordinators and demonstrates their robustness concerning output-tracking errors. The concept of ISS is utilized to characterize this robustness. With the information exchange of topology \mathcal{G} , consider the following distributed optimal coordinators:

$$\dot{y}_i^r = -\nabla c_i(y_i) - \sum_{j \in \mathcal{N}} a_{ij}(q_i - q_j), \quad (4.27)$$

$$\dot{q}_i = \mu \sum_{j \in \mathcal{N}} a_{ij}(y_i^r - y_j^r), \quad (4.28)$$

where the reference signal $y_i^r \in \mathbb{R}^{n_y}$ is intended for the output of agent i to track in the fast timescale τ . An auxiliary state $q_i \in \mathbb{R}^{n_y}$ is introduced in the fast timescale τ , while a_{ij} represents nonnegative constants defined by the weighted digraph \mathcal{G} , and $\mu > 0$ is a designated parameter for design purposes.

Denote $y = [y_1^T, \dots, y_N^T]^T$, $y^r = [y_1^{rT}, \dots, y_N^{rT}]^T$, $q = [q_1^T, \dots, q_N^T]^T$, $\Delta_c(y) = [\nabla^T c_1(y_1), \dots, \nabla^T c_N(y_N)]^T$, and $\Delta_c(y^r) = [\nabla^T c_1(y_1^r), \dots, \nabla^T c_N(y_N^r)]^T$. Then, (4.27) and (4.28) can be rewritten as

$$\dot{y}^r = -\Delta_c(y^r) - L \otimes I_{n_y} q + (\Delta_c(y^r) - \Delta_c(y)), \quad (4.29)$$

$$\dot{q} = \mu L \otimes I_{n_y} y^r, \quad (4.30)$$

where $(\Delta_c(y^r) - \Delta_c(y))$ represents the influence of the output tracking error $y - y^r$ of the agents.

The following proposition gives the equilibrium of (4.29) and (4.30) with $y \equiv y^r$.

Proposition 4.1. *With Assumptions 2.2 and 2.3 satisfied, (4.29) and (4.30) with $y \equiv y^r$ admits a unique equilibrium $[y_0^{rT}, \hat{q}_0^T]^T$ defined by*

$$L \otimes \hat{q}_0 = -\Delta_c(\mathbf{1}_N \otimes y^*), \quad (4.31)$$

$$y_0^r = \mathbf{1}_N \otimes y^*. \quad (4.32)$$

Denote $\bar{y} = y^r - y_0^r$ and $\bar{q} = \hat{q} - \hat{q}_0$, where y_0^r and \hat{q}_0 are defined by (4.31) and (4.32). Then, (4.29) and (4.30) can be rewritten as

$$\dot{\bar{y}} = -(\Delta_c(y^r) - \Delta_c(y_0^r)) - L \otimes I_{n_y} \bar{q} + (\Delta_c(y^r) - \Delta_c(y)), \quad (4.33)$$

$$\dot{\bar{q}} = \mu L \otimes I_{n_y} \bar{y}. \quad (4.34)$$

Throughout the rest of the paper, we use the notation $\bar{y}_i = y_i^r - y^*$ for $i \in \mathcal{N}$. By using the definitions of y_0^r in (4.32) and \bar{y}_i above, we have $\bar{y} = [\bar{y}_1^T, \dots, \bar{y}_N^T]^T$. Also, we use $\tilde{y} = [\tilde{y}_1^T, \dots, \tilde{y}_N^T]^T$ with $\tilde{y}_i = y_i - y_i^r$ for $i \in \mathcal{N}$ to represent the reference-tracking errors. For convenience of discussions, denote $Z = [\bar{y}^T, \bar{q}^T]^T$.

The following proposition employs ISS to formulate the robustness of (4.33) and (4.34) with respect to the reference-tracking errors \tilde{y} .

Proposition 4.2. *With Assumptions 2.2 and 2.3 satisfied, (4.33) and (4.34) are ISS with \tilde{y} as the input and Z as the state. Specifically, there exist constants $k_1 > 0$, $k_2 > 0$, and $0 < \epsilon < 1$ such that*

$$P = \begin{bmatrix} \mu k_1 I_N & k_2 L \\ k_2 L^T & k_1 I_N \end{bmatrix}, \quad Q = \begin{bmatrix} Q_1 & 0 \\ 0 & Q_2 \end{bmatrix},$$

where

$$\begin{aligned} Q_1 &= (2\mu k_1 \omega - \mu k_1 \epsilon - k_2 \vartheta^2) I_N - 2\mu k_2 L L^T, \\ Q_2 &= k_2 (1 - \epsilon) L^T L \end{aligned}$$

are positive definite, and

$$V_0(Z) = Z^T (P \otimes I_{n_y}) Z \quad (4.35)$$

is an ISS-Lyapunov function satisfying

$$\dot{V}_0(Z) \leq -b_1 V_0(Z) + b_2 |\tilde{y}|^2 \quad (4.36)$$

with $b_1 = \lambda_{\min}(Q)/\lambda_{\max}(P)$, $b_2 = (\mu k_1 + k_2)\vartheta^2/\epsilon$.

Proof. The similar conclusion has been proven in [26], so specific evidence can be found in [26]. \square

4.4. A small-gain condition with singular perturbation for optimal output consensus

In this subsection, we assume that the state of each controlled agent is bounded and convergent. The paper employs the ISS property to characterize convergence: if the reference signal is constant or converging, the output converges to the reference signal; If the reference signal is time-varying, then all states remain bounded.

In Theorems 4.1–4.4, we conclude that the slow and fast subsystems (3.10) and (3.11) can achieve ISS with respect to \dot{y}^r as the input by the sliding mode controller. Therefore, there exists an ISS-Lyapunov function $V_i(X_i) : \mathbb{R}^{n_{x_i}} \times \mathbb{R}^{n_y} \rightarrow \mathbb{R}$ such that

$$\underline{\alpha}_i(|X_i|) \leq V_i(X_i) \leq \bar{\alpha}_i(|X_i|), \quad (4.37)$$

$$V_i(X_i) \geq \max_{i \in \mathcal{N}} \{\gamma_{V_i}^{\dot{y}^r}(|y_i^r|)\} \Rightarrow \nabla V_i(X_i) F_i(X_i, y_i^r) \leq -\alpha_i(V_i(X_i)), \quad (4.38)$$

where $X_i = [x_i^T, z_i^T]^T$, $\underline{\alpha}_i$, $\bar{\alpha}_i$, and $\gamma_{V_i}^{\dot{y}^r}$ are class \mathcal{K}_∞ functions, and α_i is a continuous and positive definite function. $F_i(X_i, y_i^r)$ denotes the dynamics of the slow and fast subsystems.

Theorem 4.5. Consider the closed-loop singular perturbation system composed of (2.1)–(2.3), composite sliding mode controller (2.9) and (2.10), and distributed optimal coordinators (4.27) and (4.28). Under Assumptions 2.1–2.3, all the signals in the system are bounded, and the distributed optimization objective (2.4) is achieved if the following small-gain conditions are satisfied:

$$\gamma_{V_i}^{\dot{y}^r} \circ \gamma_{V_0}^{\tilde{y}} \leq Id, \quad (4.39)$$

where $\gamma_{V_0}^{\tilde{y}}(s) = \frac{b_2}{\sigma b_1} s^2$ for $s \in \mathbb{R}^+$.

Proof. Based on Proposition 4.2, we have

$$\dot{V}_0(Z) \leq -(1 - \sigma)b_1 V_0(Z) - \sigma b_1 V_0(Z) + b_2 |\tilde{y}|^2, \quad (4.40)$$

where $0 < \sigma < 1$ is a constant.

Therefore, we have

$$V_0(Z) \geq \gamma_{V_0}^{\tilde{y}_i}(|\tilde{y}_i|) \Rightarrow \nabla V_0(Z)F_Z(Z, \tilde{y}_i) \leq -(1 - \sigma)b_1 V_0(Z), \tag{4.41}$$

where $F_Z(Z, \tilde{y}_i)$ denotes the dynamics of distributed optimal coordinators.

The entire system can be considered as an interconnected system, as shown in Figure 4. Properties (4.41) and (4.38) characterize the gain properties between $V_0(Z)$ and $V_i(X_i)$. Choose $\gamma_{V_i}^{\tilde{y}_i} \in \mathcal{K}_\infty$ to satisfy the nonlinear small-gain condition (4.39). Then, we construct a Lyapunov function for the entire system as

$$V(X, Z) = \max_{i \in N} \{V_0(Z), \sigma_i(V_i(X_i))\}, \tag{4.42}$$

where $X = [X_1^T, X_2^T, \dots, X_N^T]^T$, which satisfies

$$\dot{V}(X, Z) \leq -\alpha_V \bar{V}(X, Z) \tag{4.43}$$

for any $(x_i(0), z_i(0), y_i^r(0), q_i(0))$ and for almost all $t \geq 0$, where σ_i is of class \mathcal{K}_∞ and continuously differentiable on $(0, \infty)$, and satisfies $\sigma_i > \gamma_{V_i}^{\tilde{y}_i}$ and $\sigma_i \circ \gamma_{V_0}^{\tilde{y}_i} < \text{Id}$,

$$\alpha_V = \frac{1}{3} \min_{i \in N} \{\sigma_i^d(\sigma_i^{-1}(s))\alpha_i(\sigma_i^{-1}(s))\} \tag{4.44}$$

with

$$\sigma_i^d = \begin{cases} \frac{\partial \sigma_i(s)}{\partial s}, & s > 0, \\ \lim_{s \rightarrow 0^+} \frac{\partial \sigma_i(s)}{\partial s}, & s = 0. \end{cases} \tag{4.45}$$

This means that the closed-loop system is asymptotically stable at the equilibrium, i.e., $\lim_{t \rightarrow +\infty} |y_i(t) - y^*| = 0$. □

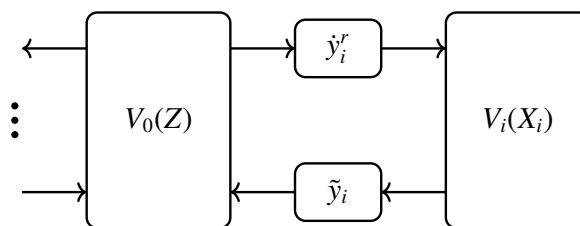


Figure 4. The interconnections within the controlled system.

5. Example

This section delves into the intricate process of designing distributed optimal coordinators and sliding mode controllers tailored specifically for a multi-agent system comprising five agents, i.e., $N = 5$. The dynamics of each agent are described as follows:

$$\dot{x}_i = x_i^2 + \sin(x_i)z_i + u_i, \tag{5.1}$$

$$\varepsilon \dot{z}_i = 2x_i^3 - x_i z_i + u_i, \quad (5.2)$$

$$y_i = x_i \quad (5.3)$$

for $i = 1, 2, 3, 4, 5$, where $\varepsilon = 0.1$, x_i and z_i denote the system state, and y_i denotes the output, respectively.

In Figure 5, the digraph and the adjacency matrix are presented, which mean that Assumption 2.3 is satisfied. The local objective functions are chosen as

$$c_i(r) = 0.1(r - 1)^2 \quad (5.4)$$

for $i = 1, 2, 3, 4, 5$, and we can check that Assumption 2.2 is satisfied with $\omega = 0.2$ and $\vartheta = 0.2$. The optimal solution of the optimization problem defined by (2.4) is $y^* = 3$. In addition, the Assumption 2.1 can be easily verified to hold.

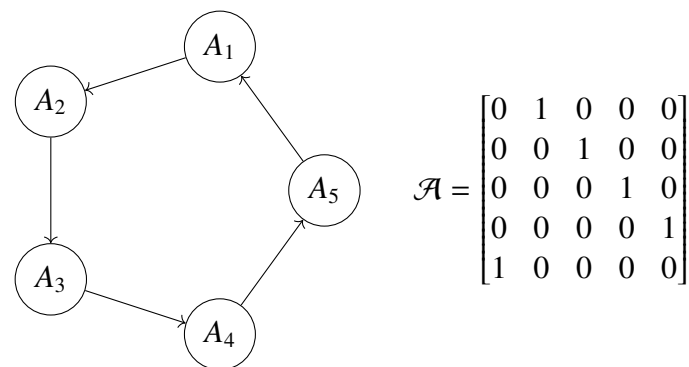


Figure 5. The information exchange digraph and the adjacency matrix.

For the design of fast-slow sliding mode controller, the parameters are set as $k_{si} = 0.2$, $k_{fi} = 0.5$, $\beta_i = 0.1$ and $\delta_i = 3$ for $i = 1, 2, 3, 4, 5$. The distributed optimal coordinators (4.27) and (4.28) are designed with $\mu = 0.8$. Based on Proposition 4.2 and Theorem 4.2, $k_1 = 264$, $k_2 = 18$, $\epsilon = 0.5$, $b_1 = 0.07$, $b_2 = 18.24$. We set as $\sigma = 12$ and $\gamma_{V_i}^{\bar{y}_i}(s) = 0.001 \sqrt{s}$, then, $\gamma_{V_0}^{\bar{y}_i}(s) = 21.7143s^2$ and (4.39) is satisfied.

A numerical simulation is addressed to verify the proposed design with initial state $x_i(0) = [0, 0.1, 0.2, 0.3, 0.4]^T$, $z_i(0) = [-0.5, -0.4, -0.3, -0.2, -0.1]^T$, $y_i^r = [0, 0.1, 0.1, 0.2, 0.2]^T$, $q_i(0) = [0, 0, 0.1, 0.1, 0]^T$. Under the aforementioned design and initial conditions, the simulation results are depicted in Figures 6–11. Figure 6 illustrates the convergence of the output of the controlled system to the optimal value point of the global objective function. Figures 7 and 8 present the tracking errors of the control inputs of controlled system and the reference signals generated by the optimizer, respectively. As shown in Figures 8 and 11, it can be observed that as ε varies from 0.1 to 0.9, the convergence of tracking error remains unchanged, but the convergence time increases. From the simulation results, it can be observed that the proposed method successfully drives the output of the singular perturbed multi-agent system to the optimal value point of the objective function.

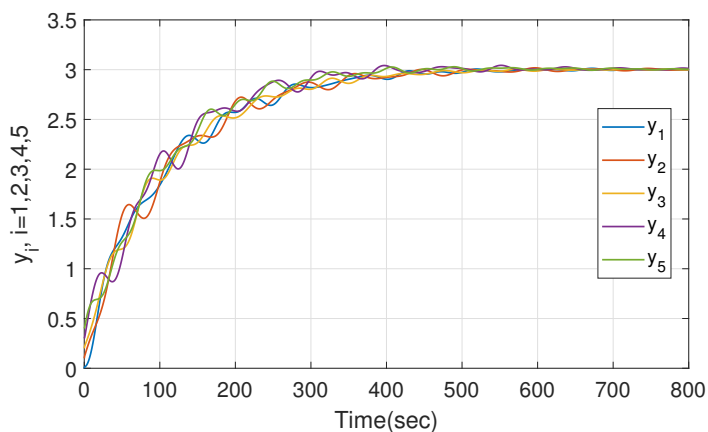


Figure 6. Convergence of the outputs y_i of the controlled singular perturbed agents.

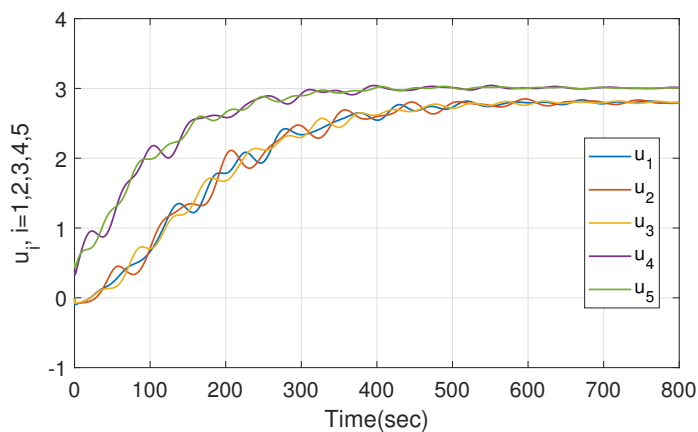


Figure 7. Control inputs u_i of the controlled singular perturbed agents.

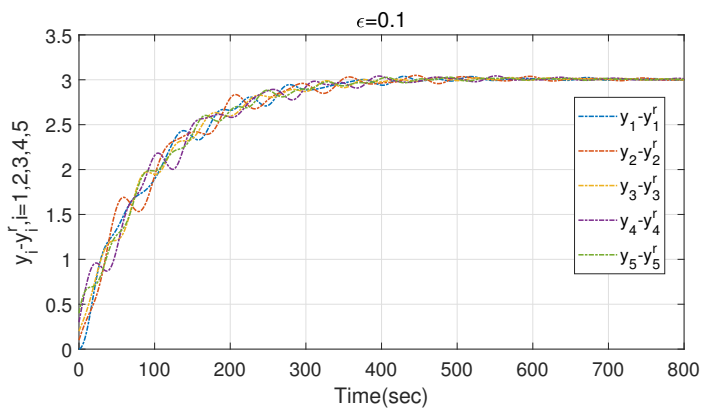


Figure 8. Reference-tracking capability of controlled singular perturbed agents.

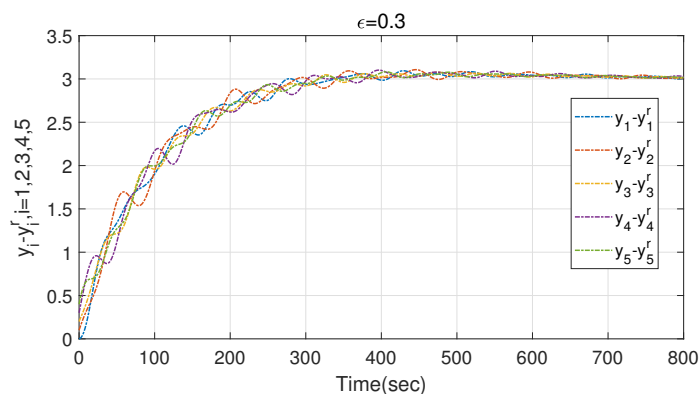


Figure 9. Reference-tracking capability of controlled singular perturbed agents, when $\epsilon = 0.3$.

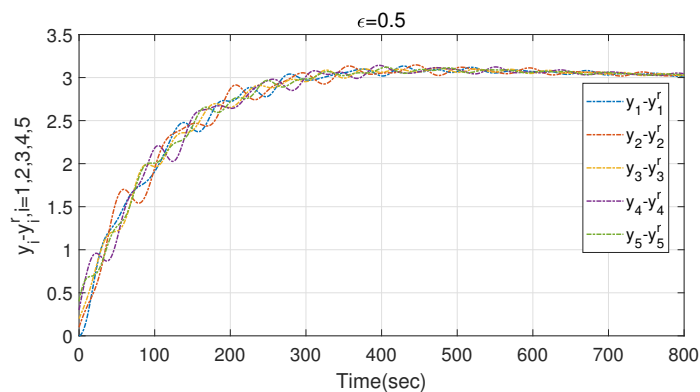


Figure 10. Reference-tracking capability of controlled singular perturbed agents, when $\epsilon = 0.5$.

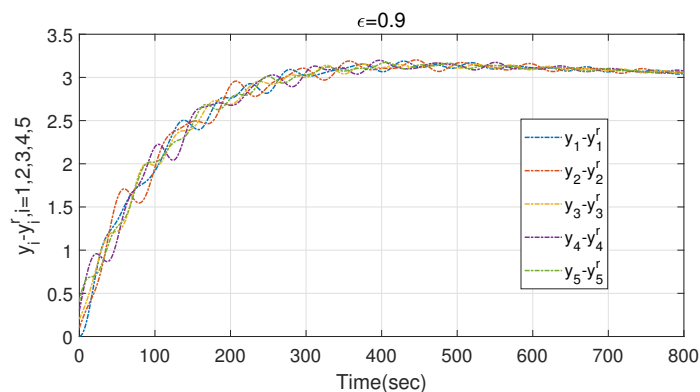


Figure 11. Reference-tracking capability of controlled singular perturbed agents, when $\epsilon = 0.9$.

6. Conclusions

This paper presents a comprehensive exploration of distributed optimization within nonlinear singular perturbation systems. Initially, the singular perturbation system is dissected into fast and slow subsystems, laying the groundwork for subsequent methodologies. Robustness in tracking reference signals is ensured through the implementation of fast-slow sliding mode controllers. Moreover, to mitigate errors between reference signals and optimal values, a distributed optimizer is proposed to generate reference signals, ensuring robustness in the face of uncertainties. The stability of the entire closed-loop system is rigorously scrutinized using the small-gain theorem, bolstering the theoretical underpinnings of the proposed framework. A numerical example is provided to substantiate the efficacy of the proposed approach. Through this study, significant strides have been made in addressing the formidable challenges inherent in distributed optimization within nonlinear singular perturbation systems, laying a solid foundation for future advancements in this field.

The future of networked sliding mode control is promising, with numerous advancements expected in robustness, communication integration, cybersecurity, distributed control, artificial intelligence integration, and practical applications. These developments will pave the way for more resilient, efficient, and intelligent control systems, driving innovation across various industries.

Author contributions

Qian Li: Validation, Visualization, Writing-original draft, Methodology, Formal analysis; Zhenghong Jin: Writing-review & editing, Supervision, Validation, Visualization, Conceptualization; Linyan Qiao: Investigation, Data curation; Aichun Du: Resources, Software; Gang Liu: Funding acquisition, Project administration. All authors have read and approved the final version of the manuscript for publication.

Use of AI tools declaration

The authors declare they have not used artificial intelligence (AI) tools in the creation of this article.

Acknowledgments

This work was supported by National Natural Science Foundation of China under Grant U1911401, Key scientific research project of colleges and universities in Henan Province (No. 22B46003) and Henan Province Key R&D and Promotion Special (Science and Technology Research) Project (No. 212102210046).

Conflict of interest

The authors declare no conflicts of interest.

References

1. L. Y. Cao, H. M. Schwartz, Complementary results on the stability bounds of singularly perturbed systems, *IEEE Trans. Automat. Control*, **49** (2004), 2017–2021. <https://doi.org/10.1109/TAC.2004.837546>
2. T. Nguyen, Z. Gajic, Finite Horizon optimal control of singularly perturbed systems: a differential Lyapunov equation approach, *IEEE Trans. Automat. Control*, **55** (2010), 2148–2152. <https://doi.org/10.1109/TAC.2010.2051187>
3. C. X. Qiang, J. P. Sun, Y. H. Zhao, Exponential stability analysis for nonlinear time-varying perturbed systems on time scales, *AIMS Math.*, **8** (2023), 11131–11150. <https://doi.org/10.3934/math.2023564>
4. J. X. Chen, C. X. He, Modeling, fault detection, and fault-tolerant control for nonlinear singularly perturbed systems with actuator faults and external disturbances, *IEEE Trans. Fuzzy Syst.*, **30** (2022), 3009–3022. <https://doi.org/10.1109/TFUZZ.2021.3099470>
5. H. Shen, F. Li, Z. G. Wu, J. H. Park, V. Sreeram, Fuzzy-model-based nonfragile control for nonlinear singularly perturbed systems with semi-Markov jump parameters, *IEEE Trans. Fuzzy Syst.*, **26** (2018), 3428–3439. <https://doi.org/10.1109/TFUZZ.2018.2832614>
6. E. Fridman, Effects of small delays on stability of singularly perturbed systems, *Automatica*, **38** (2002), 897–902. [https://doi.org/10.1016/S0005-1098\(01\)00265-5](https://doi.org/10.1016/S0005-1098(01)00265-5)
7. M. Corless, L. Glielmo, On the exponential stability of singularly perturbed systems, *SIAM J. Control Optim.*, **30** (1992), 1338–1360. <https://doi.org/10.1137/0330071>
8. A. Saberi, H. Khalil, Stabilization and regulation of nonlinear singularly perturbed systems—composite control, *IEEE Trans. Automat. Control*, **30** (1985), 739–747. <https://doi.org/10.1109/TAC.1985.1104064>
9. H. Wang, C. Y. Yang, X. M. Liu, L. N. Zhou, Neural-network-based adaptive control of uncertain MIMO singularly perturbed systems with full-state constraints, *IEEE Trans. Neural Netw. Learn. Syst.*, **34** (2023), 3764–3774. <https://doi.org/10.1109/TNNLS.2021.3123361>
10. F. Li, W. X. Zheng, S. Y. Xu, Finite-time fuzzy control for nonlinear singularly perturbed systems with input constraints, *IEEE Trans. Fuzzy Syst.*, **30** (2022), 2129–2134. <https://doi.org/10.1109/TFUZZ.2021.3072737>
11. H. Shen, Y. Wang, J. Wang, J. H. Park, A fuzzy-model-based approach to optimal control for nonlinear Markov jump singularly perturbed systems: a novel integral reinforcement learning scheme, *IEEE Trans. Fuzzy Syst.*, **31** (2023), 3734–3740. <https://doi.org/10.1109/TFUZZ.2023.3265666>
12. H. Shen, C. J. Peng, H. C. Yan, S. Y. Xu, Data-driven near optimization for fast sampling singularly perturbed systems, *IEEE Trans. Automat. Control*, 2024, 1–6. <https://doi.org/10.1109/TAC.2024.3352703>
13. E. S. Tognetti, T. R. Calliero, I. C. Morarescu, J. Daafouz, Synchronization via output feedback for multi-agent singularly perturbed systems with guaranteed cost, *Automatica*, **128** (2021), 109549. <https://doi.org/10.1016/j.automatica.2021.109549>

14. J. Cortés, F. Bullo, Coordination and geometric optimization via distributed dynamical systems, *SIAM J. Control Optim.*, **44** (2005), 1543–1574. <https://doi.org/10.1137/S0363012903428652>
15. P. Colli, G. Gilardi, J. Sprekels, Distributed optimal control of a nonstandard nonlocal phase field system, *AIMS Math.*, **1** (2016), 225–260. <https://doi.org/10.3934/Math.2016.3.225>
16. B. M. Huang, Y. Zou, Z. Y. Meng, W. Ren, Distributed time-varying convex optimization for a class of nonlinear multiagent systems, *IEEE Trans. Automat. Control*, **65** (2020), 801–808. <https://doi.org/10.1109/TAC.2019.2917023>
17. Y. K. Zheng, Y. X. Li, C. K. Ahn, Adaptive fuzzy distributed optimization for uncertain nonlinear multiagent systems, *IEEE Trans. Fuzzy Syst.*, **32** (2024), 1862–1872. <https://doi.org/10.1109/TFUZZ.2023.3337170>
18. G. Carnevale, G. Notarstefano, Nonconvex distributed optimization via Lasalle and singular perturbations, *IEEE Control Syst. Lett.*, **7** (2023), 301–306. <https://doi.org/10.1109/LCSYS.2022.3187918>
19. L. Zhang, S. Liu, Distributed average consensus of stochastic singularly perturbed systems, *IEEE Trans. Control Netw. Syst.*, **10** (2023), 1913–1924. <https://doi.org/10.1109/TCNS.2023.3256271>
20. Z. P. Jiang, A. R. Teel, L. Praly, Small-gain theorem for ISS systems and applications, *Math. Control Signals Syst.*, **7** (1994), 95–120. <https://doi.org/10.1007/BF01211469>
21. A. R. Teel, A nonlinear small gain theorem for the analysis of control systems with saturation, *IEEE Trans. Automat. Control*, **41** (1996), 1256–1270. <https://doi.org/10.1109/9.536496>
22. Z. P. Jiang, I. M. Y. Mareels, Y. Wang, A Lyapunov formulation of the nonlinear small-gain theorem for interconnected ISS systems, *Automatica*, **32** (1996), 1211–1215. [https://doi.org/10.1016/0005-1098\(96\)00051-9](https://doi.org/10.1016/0005-1098(96)00051-9)
23. Z. H. Jin, Z. X. Wang, Input-to-state stability of the nonlinear singular systems via small-gain theorem, *Appl. Math. Comput.*, **402** (2021), 126171. <https://doi.org/10.1016/j.amc.2021.126171>
24. T. Tatarenko, B. Touri, Non-convex distributed optimization, *IEEE Trans. Automat. Control*, **62** (2017), 3744–3757. <https://doi.org/10.1109/TAC.2017.2648041>
25. Z. H. Jin, C. K. Ahn, J. W. Li, Momentum-based distributed continuous-time nonconvex optimization of nonlinear multi-agent systems via timescale separation, *IEEE Trans. Netw. Sci. Eng.*, **10** (2023), 980–989. <https://doi.org/10.1109/TNSE.2022.3225409>
26. T. F. Liu, Z. Y. Qin, Y. G. Hong, Z. P. Jiang, Distributed optimization of nonlinear multiagent systems: a small-gain approach, *IEEE Trans. Automat. Control*, **67** (2022), 676–691. <https://doi.org/10.1109/TAC.2021.3053549>
27. Q. S. Liu, J. Wang, A second-order multi-agent network for bound constrained distributed optimization, *IEEE Trans. Automat. Control*, **60** (2015), 3310–3315. <https://doi.org/10.1109/TAC.2015.2416927>
28. J. Wang, K. M. Tsang, Second-order sliding mode controllers for nonlinear singular perturbation systems, *ISA Trans.*, **44** (2005), 117–129. [https://doi.org/10.1016/S0019-0578\(07\)60049-4](https://doi.org/10.1016/S0019-0578(07)60049-4)
29. J. Alvarez-Gallegos, G. Silva-Navarro, Two-time scale sliding-mode control for a class of nonlinear systems, *Int. J. Robust Nonlinear Control*, **7** (1997), 865–879.

30. T. F. Liu, Z. P. Jiang, A small-gain approach to robust event-triggered control of nonlinear systems, *IEEE Trans. Automat. Control*, **60** (2015), 2072–2085. <https://doi.org/10.1109/TAC.2015.2396645>
31. Y. T. Chang, Adaptive sliding mode control of multi-input nonlinear systems with perturbations to achieve asymptotical stability, *IEEE Trans. Automat. Control*, **54** (2009), 2863–2869. <https://doi.org/10.1109/TAC.2009.2033748>
32. X. Y. Zhang, H. Y. Su, R. Q. Lu, Second-order integral sliding mode control for uncertain systems with control input time delay based on singular perturbation approach, *IEEE Trans. Automat. Control*, **60** (2015), 3095–3100. <https://doi.org/10.1109/TAC.2015.2411991>
33. C. A. Martinez-Fuentes, R. Seeber, L. Fridman, J. A. Moreno, Saturated Lipschitz continuous sliding mode controller for perturbed systems with uncertain control coefficient, *IEEE Trans. Automat. Control*, **66** (2021), 3885–3891. <https://doi.org/10.1109/TAC.2020.3034872>



AIMS Press

© 2024 the Author(s), licensee AIMS Press. This is an open access article distributed under the terms of the Creative Commons Attribution License (<https://creativecommons.org/licenses/by/4.0>)